Preprints (www.preprints.org) | NOT PEER-REVIEWED | Posted: 14 July 2022 doi:10.20944/preprints202207.0215.v1

Assembly and disassembly mechanics of a spherical snap fit

Xiao-Lin Guo[1] and Bo-Hua Sun *[1]

[1]School of Civil Engineering & Institute of Mechanics and Technology
Xi'an University of Architecture and Technology, Xi'an 710055, China

The snap fit is a common mechanical mechanism. We have studied the spherical snap fit carefully for its physical asymmetry which is easy to assemble but difficult to disassemble. Because of the complexity of spherical structure, it is difficult to get a theoretical formula to describe its physical asymmetry. In this paper, through the method of combining theory, simulation and experiment, and based on the theoretical results of cylindrical snap fit obtained in the early stage, the pushing assembly and pulling disassembly of spherical snap fit are studied, we not only propose the theoretical formula of spherical snap fit, but also further verify its correctness. This research provides theoretical support and basis for the optimization design and further research of snap fit.

I. INTRODUCTION

Although we often hear the "click" sound of the snap fit in our daily lives, there is very little research on the scientific mechanism of the snap fit mechanism. The snap fit appears everywhere in our daily lives because it is simple and reusable [1–13]. Two objects can be directly connected without welding, bolts, glue, or other means, and they can be assembled and disassembled repeatedly [1, 12, 13]. From receptor ligand interaction [2] in biochemistry to spacecraft docking [3], as well as zippers, Lego blocks, water pipe clamps, head massager claw etc., which are common in life, all use the principle of snap fit. Although the snap fit is not an uncommon, it uses a basic physical mechanism, mechanical asymmetry in that it is easy to assemble but difficult to disassemble.

Snap fits are distinguished according to their shapes, and the common types of snap fits include cantilever snap fit [1, 5], ring snap fit,spherical snap fit, etc. Among them, the spherical snap fit is widely used in the connection part because of its bidirectional freedom and difficult to disassemble snap fit (that is, the mounting force and disassembly force required by the connection are both large), as shown in Fig. (1) .

FIG. 1: Spherical snap fit

Spherical shapes have bi-directional curvature, and curvature has a great influence on forces, as shown in Fig. (2), just one curvature difference can change the load capacity by 100 times [6]. Therefore, the spherical snap fit should have greater assembly and disassembly force than the corresponding cylindrical snap fit.

FIG. 2: The effect of curvature on force [6]

The snap fit assembly and disassembly process from the physical point of view is the interaction between geometry, friction and bending elasticity, and the assembly and disassembly of these two processes is asymmetric, that is, easy to assemble but difficult to disassemble [7–11]. The study of snap fits helps to understand the asymmetry (i.e. easy to assemble but difficult to disassemble) process, in 2020, Yoshida and Wada [12] cite creative-

*Corresponding author: Bo-Hua Sun, email: sunbohua@xauat.edu.cn

© 2022 by the author(s). Distributed under a Creative Commons CC BY license.

Preprints (www.preprints.org) | NOT PEER-REVIEWED | Posted: 14 July 2022 doi:10.20944/preprints202207.0215.v1

ly study the assembly and disassembly mechanics of the cylindrical snap fit in detail, and give some basic relations and phase diagrams of pushing assembly and pulling disassembly problems of the cylindrical snap fit, which opens a new topic of accurately predicting the mechanism of the snap fit from a scientific point of view. Based on the research of Yoshida and Wada [12], this paper studies the reliability of Yoshida and Wada's approximation and presents a higher order approximation.

For the spherical snap fit, since its Gauss curvature is not zero (while the Gauss curvature of the cylindrical snap fit is zero), it can be predicted that the assembly and disassembly force of the spherical snap fit should be larger than that of the cylindrical snap fit. However, there is no relevant research on the quantitative prediction of the assembly and disassembly force of the spherical snap fit. This question is the research purpose of this paper.

Specifically, we first introduced the assembly and disassembly mechanism of spherical snap fit, then deduced its theoretical model, obtained the theoretical formula of spherical snap fit with friction; Finite element simulation is carried out on pushing assembly and pulling disassembly process of two types of snap fits, and then we use 3D printer microcomputer control electronic universal testing machine (E43.1044) for experimental verification. In order to have a deeper understanding of physics, we carry out experimental analysis and comparison, and finally give a conclusion.

II. ASSEMBLY AND DISASSEMBLY MECHANISM AND FINITE ELEMENT SIMULATION OF SINGLE-JAW SPHERICAL SNAP FIT

As shown in Figs. (3), we consider hyperbolic semi-cylindrical shell with radius of R_s, thickness of t, length of L, and opening angle of Φ. It is pushed onto the surface of a rigid sphere with a radius R_c to form a single-jaw spherical snap fit.

According to the radius ratio α, opening angle ϕ, and material parameters (friction coefficient $\mu = 0.21$) of the snap fit in Yoshida and wada[12], we calculated the single jaw spherical snap fit model with 10 different opening angles by using the finite element software ABAQUS, as shown in Table I. The finite element model is shown in Fig. 4.

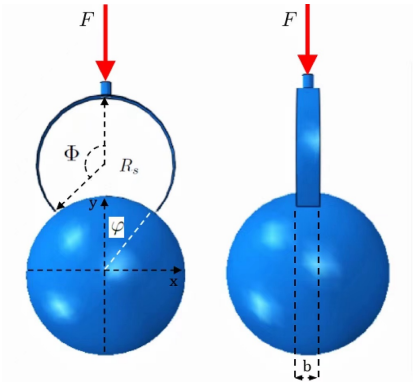

FIG. 3: Single-jaw spherical snap fit

TABLE I: Parameters of single jaw spherical snap fit

Radius ratio	Length	Thickness	Opening angle
α	L(mm)	t(mm)	$\Phi(rad)$
1.14	8	0.3	1.9
1.14	8	0.3	2.0
1.14	8	0.3	2.1
1.14	8	0.3	2.2
1.14	8	0.3	2.3
1.14	8	0.3	2.4
1.14	8	0.3	2.5
1.14	8	0.3	2.6
1.14	8	0.3	2.7
1.14	8	0.3	2.8

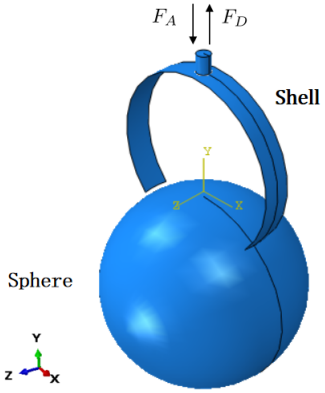

FIG. 4: Finite element model

The simulation process was divided into two steps: assembly and disassembly. During the assembly process, the shell moved down at a speed of 5 mm/s until the top of the shell touched the spheroidal surface. After 1 s, the housing moved up at the same speed of 5 mm/s (disassembly process).

Due to the interaction of the initial opening angle ϕ,

Preprints (www.preprints.org) | NOT PEER-REVIEWED | Posted: 14 July 2022 doi:10.20944/preprints202207.0215.v1

radius ratio α and friction coefficient μ of the snap fit, it can be seen from the finite element simulation results that the snap fit with different parameters corresponds to different physical phenomena, namely sliding installation and jumping installation [16]. Accordingly, we can still divide the spherical snap fit into two types: Type I snap-fit (small deflection) and Type II snap-fit (large deflection). The assembly process of the two types of single-jaw spherical snaps is shown in Fig. 5 and Fig.6.

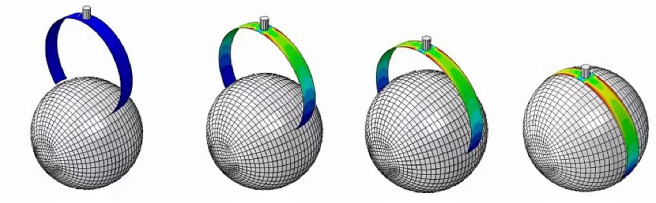

FIG. 5: Type I snap-fit

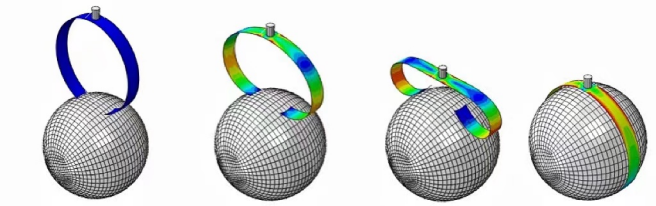

FIG. 6: Type II snap-fit

In order to study the mechanical asymmetry of spherical buckle in a more detailed way, we take the opening Angle of Type I snap-fit $\Phi = 2.3\ rad$ and the opening Angle of Type II snap-fit $\Phi = 2.7\ rad$ as examples. The measured force F is displayed in units of R^2/B and draw a forcing-displacement diagram, as shown in Fig. 7.

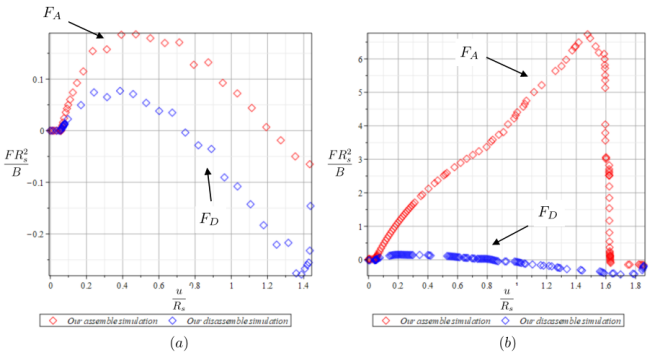

FIG. 7: Finite element simulation diagram of snap fit assembly and disassembly: (a) Type I snap-fit and (b) Type II snap-fit.

It can be seen that the finite element simulation diagram of single jaw spherical snap fit is exactly the same as that of cylindrical snap fit. It is further proved that the results of previous research on the cylindrical snap fit are correct, and the results are specific and universal.

III. MECHANICAL FITTING THEORY OF ASSEMBLY AND DISASSEMBLY OF SINGLE-JAW SPHERICAL SNAP FIT

In order to further study the spherical snap fit, based on our previous research on the cylindrical snap fit, the finite element method is used to compare and simulate the single-jaw spherical snap fit and the cylindrical snap fit. When the single arm length of the snap fit is b, the difference between the spherical snap fit and the cylindrical snap fit is that the spherical snap fit is affected by the section curvature. According to the above mentioned parameters of single-jaw spherical snap fit, the corresponding cylindrical snap fit is established, as shown in Fig. (8).

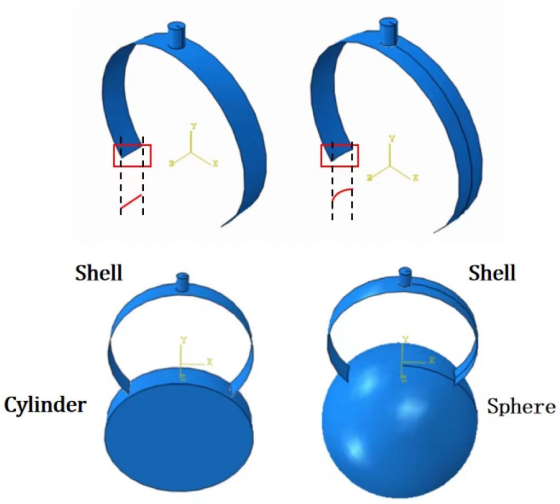

FIG. 8: Comparison of cylindrical and single jaw spherical snap fits

We compare the assembly force and disassembly force of Type I single-jaw spherical snap fit and Type I cylindrical snap fit by finite element method. The measured force F is displayed in units R^2/B. As shown in Fig. (9).

It is obvious that the assembling force F_A and disassembling force F_D of single-jaw spherical snap fit are

Preprints (www.preprints.org) | NOT PEER-REVIEWED | Posted: 14 July 2022 doi:10.20944/preprints202207.0215.v1

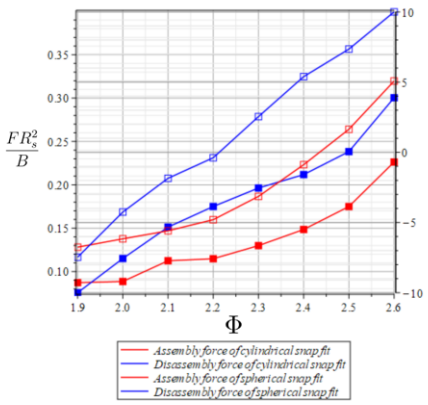

FIG. 9: Comparison diagram of FEM

obviously higher than that of cylindrical snap fit, which is related to the influence of curvature, but the curve trend is basically the same. Therefore, under the condition of small deformation (Type I snap-fit), $2.0\ rad < \Phi < 2.6\ rad$, we fit the scatter diagrams of assembly force-opening angle and disassembly force-opening angle, as shown in Fig.(III) and (11), the fitting formula is obtained.

The fitting expression of assembly force of single-jaw spherical snap fit is

$$\frac{F_A R_s^2}{B} \approx C f_A. \tag{1}$$

where C is a constant and the assembly force ratio of the cylindrical snap fit is

$$f_A = 2\alpha K_{x\|}(\Phi) S(\alpha, \Phi, \mu) \left[1 - (\frac{\sin\Phi}{\alpha})^{2/3}\right]^{3/2}, \tag{2}$$

seeing appendix for some symbols in the formula.

The fitting expression of disassembly force of single-jaw spherical snap fit is

$$\frac{F_D R_s^2}{B} = C f_D \tag{3}$$

where the disassembly force ratio of the cylindrical snap fit is

$$f_D = 2\alpha K_{x\|}(\Phi) \frac{\sin(\Phi/\alpha) - \alpha^{-1}\sin\Phi}{K_{x\|}(\Phi)/K_{x\perp} \perp (\Phi) - g(\Phi/\alpha, -\mu)}, \tag{4}$$

and see appendix for some symbols in the formula.

By data fitting, the correction coefficient is determined approximately as $C = 2.95$. Since the coefficient C should be greater than 1, it indicates that the spherical snap fit has a greater bearing capacity than the cylindrical snap fit [12, 13], confirming our prediction in the preface. Eq. (1), (3)is similar to the formula obtained

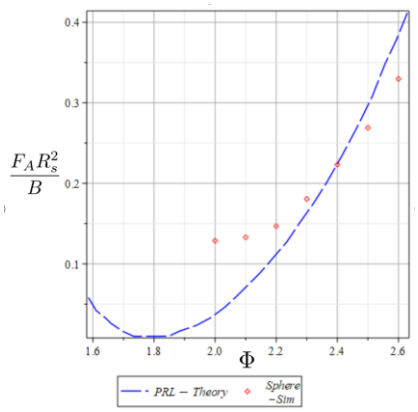

FIG. 10: Relationship between assembly force and opening angle of Type I single jaw spherical snap fit

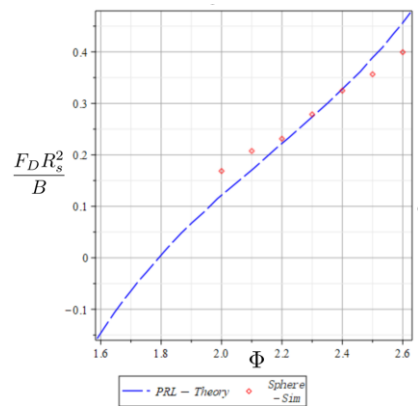

FIG. 11: Relationship between disassembly force and opening Angle of Type I single jaw spherical snap fit

by the study of the cylindrical snap fit, the only difference is that the preceding coefficient C is different. This shows that shape does not affect the physical law of mechanical asymmetry of snap fit, which further verifies the correctness of Yoshida and Wada's conclusion.

IV. ASSEMBLY AND DISASSEMBLY MECHANISM OF MULTI-JAW SPHERICAL SNAP FIT

There are many kinds of spherical snap fits, and the simplest classification is distinguished by the number of claws, as shown in Fig. (12), which are spherical snap

Preprints (www.preprints.org) | NOT PEER-REVIEWED | Posted: 14 July 2022 doi:10.20944/preprints202207.0215.v1

fits with two pairs, three pairs and four pairs of claws respectively.

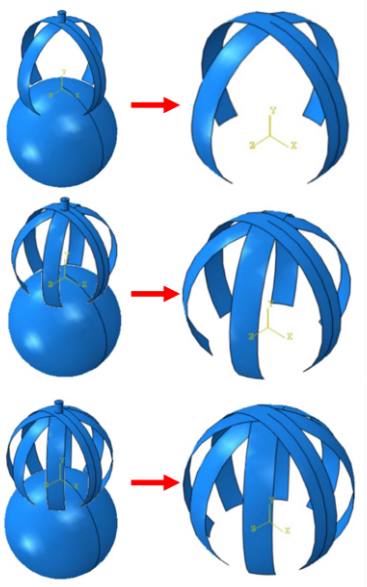

FIG. 12: multi-jaw spherical snap fit

Taking the spherical snap fit with two pairs of claws as an example, we use finite element method to study the assembly and disassembly mechanism of multi-jaw spherical snap fit, as shown in Fig. (13). We take the opening angle of Type I snap-fit $\phi = 2.3\ rad$ and Type II snap-fit $\phi = 2.7\ rad$ as examples, and the simulation process is the same as above. Due to the different initial opening angle, the snap fit corresponds to different physical phenomena, namely sliding installation and jumping installation. Accordingly, we can still divide the multi-jaw spherical snap fit into two types: Type I snap-fit (small deflection) and Type II snap-fit (large deflection). The assembly process of the two types of multi-jaw spherical snaps is shown in Fig. (14) and(15).

The measured force F is displayed in units of R^2/B and draw a forcing-displacement diagram, as shown in Fig. (16).We can clearly see that the finite element simulation results of the multi-jaw spherical snap fit are completely consistent with the finite element curve of the cylindrical snap fit.

Therefore, we can draw a conclusion that the physical law of the assembly and disassembly process of the multi-jaw spherical snap fit is consistent with that of the cylindrical snap fit, and its assembly force and disassembly force can be obtained by changing the parameter C

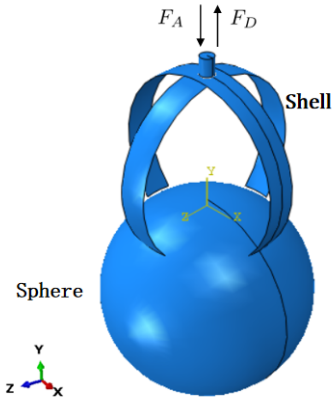

FIG. 13: Finite element model

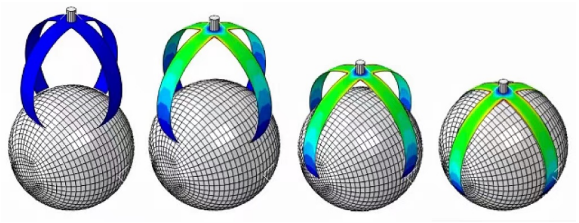

FIG. 14: Type I snap-fit

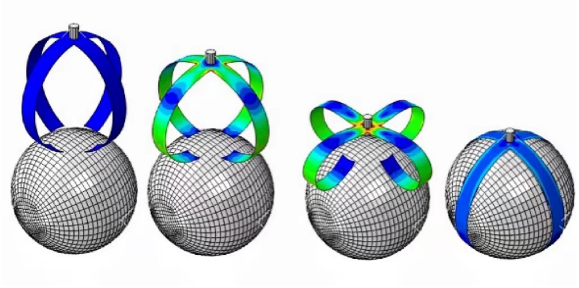

FIG. 15: Type II snap-fit

in front of Eq.1 and Eq.3 according to the number of claws. Unfortunately, we find that the force of single jaw spherical snap fit and multi-jaw spherical snap fit is not a simple multiple relationship, which may be related to the hyperbolic rate of spherical snap fit, which needs further study.

V. ASSEMBLY AND DISASSEMBLY EXPERIMENT OF SNAP FIT

In order to further prove the correctness of the finite element model of the spherical snap fit established by us,

Preprints (www.preprints.org) | NOT PEER-REVIEWED | Posted: 14 July 2022 doi:10.20944/preprints202207.0215.v1

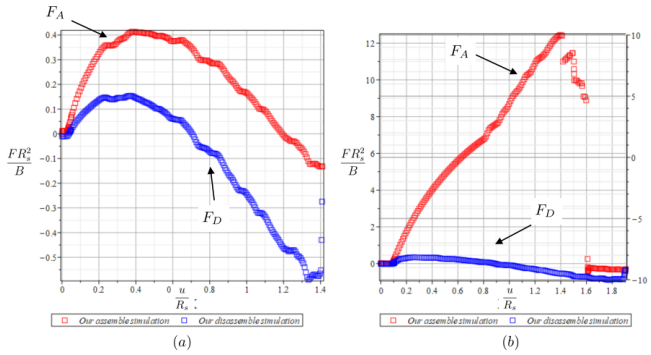

FIG. 16: Finite element simulation diagram of snap fit assembly and disassembly: (a) Type I snap-fit and (b) Type II snap-fit.

we have made a numerical comparison between simulation and experiment

The experimental model is obtained by 3D printer, and the relevant parameters of the model: $R_s = 26.3mm$, $R_c = 30mm$, $\alpha = R_c/R_s = 1.14$, $t = 1mm$, $b = 8mm$, $\Phi = 2.2\ rad$. After the model is made, use the microcomputer controlled electronic universal testing machine (E43.1044) to carry out the assembly experiment of Type I snap-fit, as shown in Fig. (**??**) (see the supplementary materials for the experimental video and simulation video).

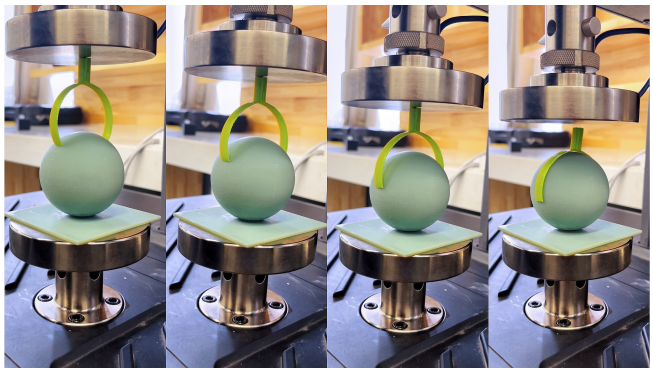

FIG. 17: Experimental set up

We established the finite element model according to the above model parameters, and drew the comparison diagram between the simulation data of the model and the experimental data, as shown in Fig. (18). According to Fig. (18), we can intuitively see that the two curves are basically consistent, and the error does not exclude factors such as friction (the friction coefficient is taken from the friction experiment) . This further proves the correctness of our finite element simulation.

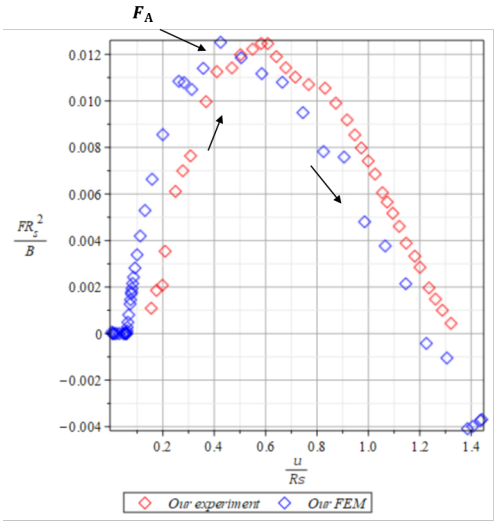

FIG. 18: Simulation data were compared with experimental data

VI. CONCLUSIONS AND OPINIONS

In this paper, firstly, the assembly and disassembly mechanism of the spherical snap fit are introduced, then the theoretical model of the spherical snap fit is deduced based on the previous research on the cylindrical snap fit, and the theoretical formula of the spherical snap fit under friction is obtained. Then the finite element simulation and experimental verification are carried out on the process of pushing assembly and pulling disassembly of two types of snap fits. The specific research conclusions are as follows: 1. The finite element simulation of single-jaw spherical snap fit is completely consistent with the finite element curve variation of cylindrical snap fit, indicating that the spherical snap fit still conforms to the mechanical asymmetry law of easy to assemble but difficult to disassemble; 2. The scatter diagram obtained by fitting the results of finite element simulation shows that the theoretical formula of spherical snap fit is similar to that of cylindrical snap fit, the only difference is that the value of coefficient C is different. This shows that shape does not affect the physical scaling law of the mechanical asymmetry of the snap fit. 3. The experimental results of mounting and disassembling of single-jaw spherical snap fit show that the snap fit force curves obtained by simulation are basically consistent with those obtained by ex-

Preprints (www.preprints.org) | NOT PEER-REVIEWED | Posted: 14 July 2022 doi:10.20944/preprints202207.0215.v1

periment, which verifies the correctness of finite element simulation and theoretical formula. 4. The multi-jaw spherical snap fit obtained by finite element simulation of single-jaw spherical snap fit still conforms to the law of mechanical asymmetry, but the snap fit force between multi-jaw spherical snap fit and single-jaw spherical snap fit is not a simple multiple relationship due to the influence of curvature and other factors, which requires to be further studied. This is another detailed study of snap fit mechanics in the context of thin structure physics [12, 13], which helps to accurately predict the assembly and disassembly forces of spherical snap fits.

Acknowledgement: The authors wish to express their appreciation to the financial support from Xian University of Architecture and Technology (Project no: 002/2040221134).

Conflict of interest The author declares that he has no known competing financial interests or personal relationships that could have appeared to influence the work reported in this paper.

Data availability The data that support the findings of this study are available from the corresponding author upon reasonable request.

Appendix

We consider a semi-cylindrical shell with radius of R_s, thickness of t, length of L, and opening angle of Φ. It is pushed onto the surface of a rigid cylinder with a radius R_c to form a simple cylindrical snap fit [12, 13], as shown in Fig. 19.

According to the interactions between the topology, bending elasticity, and friction that are characterized by the initial opening angle Φ, mismatch ratio $\alpha = R_c/R_s$, elasticity modulus E, and friction coefficient μ, the assembly process of the snap fit can be varied, corresponding to different physical phenomena.

From Yoshida and Wada [12, 13], we have the elastic coefficients is defined as

$$K_{x\parallel}(\Phi) = \left[\frac{\Phi}{2} - (\frac{3}{2}\sin\Phi - \Phi\cos\Phi)\cos\Phi\right]^{-1}, \quad (5)$$

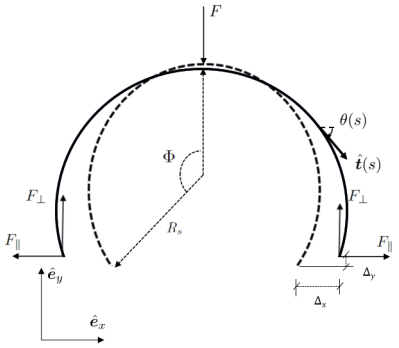

FIG. 19: Schematic diagram of cylindrical snap fit

and

$$K_{x\perp}(\Phi) = [\frac{1}{2} + (1 - \Phi\sin\Phi - \frac{3\cos\Phi}{2})\cos\Phi]^{-1} \quad (6)$$

$$g(\varphi,\mu) = \frac{\mu - \tan\varphi}{1 + \mu\tan\varphi}, \quad (7)$$

$$S(\alpha,\Phi,\mu) = \frac{\tan[(\alpha^{-1}\sin\Phi)^{1/3}]}{\frac{K_{x\parallel}(\Phi)}{K_{x\perp}(\Phi)} - g((\frac{\sin\Phi}{\alpha})^{1/3},\mu)}. \quad (8)$$

[1] Bayer Corporation, Snap-Fit Joints for Plastics: A Design Guide (Polymer Division, Pittsburgh, PA, 1996).

[2] V. T. Moy, E. L. Florin, and H. E. Gaub. Intermolecular Forces and Energies Between Ligands and Receptors. Science 266, 257 (1994).

[3] M. Romano, D. A. Friedman, and T. J. Shay. Laboratory Experimentation of Autonomous Spacecraft Approach and Docking to a Collaborative Target. J. Spacecr.Rockets 44, 164 (2007).

[4] G. Suri and A. F. Luscher. Structural Abstraction in Snap-Fit Analysis. J. Mech. Des. 122, 395 (2000).

[5] J. Ji, K.-M. Lee, and S. Zhang. The Research Works of Coulomb and Amontons and Generalized Laws of Friction. J. Mech. Des. 133, 121004 (2011).

[6] Venkadesan M, Yawar A, Eng C M, et al. Stiffness of the human foot and evolution of the transverse arch[J]. Nature, 2020, 579(7797): 97-100.

[7] R. C. Benson. The Deformation of a Thin Incomplete, Elastic Ring in a Frictional Channel. J. Appl. Mech. 48, 895 (1981).

[8] R. C. Benson. Stick/Slip Conditions for a Thin, Incomplete, Elastic Ring Impinging on a Frictional Barrier. J. Appl. Mech. 49, 231 (1982).

[9] C.-W. Liu and J.-S. Chen. Effect of friction on the planar elastica constrained inside a circular channel with clearance. Int. J. Solids Struct. 50, 270 (2013).

[10] B. Roman and A. Pocheau. Postbuckling of bilaterally constrained rect angular thin plates. J. Mech. Phys.

Preprints (www.preprints.org) | NOT PEER-REVIEWED | Posted: 14 July 2022 doi:10.20944/preprints202207.0215.v1

Solids 50, 2379 (2002).

[11] Q. S. Nguyen. Instability and Friction Instabilité et frottement. C. R. Mec. 331, 99 (2003).

[12] K. Yoshida and H. Wada, Mechanics of a snap fit, Phys.Rev.Lett. **125**, 194301 (2020)

[13] X.L. Guo and B.H. Sun, Assembly and Disassembly Mechanics of a Cylindrical Snap Fit. Preprints 2022, 2022010076 (doi: 10.20944/preprints202201.0076.v1).

[14] Suri G , Luscher A F . Evaluation Metrics for the Rating and Optimization of Snap-fits[J]. Research in Engineering Design, 2000, 12(4):191-203.

[15] A. Rafsanjani, A. Akbarzadeh, and D. Pasini. Multistable Architected Materials for Trapping Elastic Strain Energy. Adv. Mater. 27, 5931 (2015).

[16] E. Popova and V. Popov. The research works of Coulomb and Amontons and generalized laws of friction. Friction 3, 183 (2015).

[17] L. Wu, X. Xi, B. Li, and J. Zhou. Multi-Stable Mechanical Structural Materials. Adv. Eng. Mater. 20, 1700599 (2018).

[18] B. R. Mose, I.-S. Son, J.-W. Bae, H.-G. Ann, C. Y. Lee, and D.-K. Shin. Modified Analytical Method to Calculate the Assembly and Separation Forces of Cantilever Hook-Type Snap-Fit. J. Mech. Eng. Sci. 233, 5074 (2019).

[19] D. Matsumoto, T. G. Sano, and H. Wada. Pinching an Open Cylindrical Shell: Extended Deformation and its Persistence. Europhys. Lett. 123, 14001 (2018).

[20] B. Audoly and Y. Pomeau, Elasticity and Geometry (Oxford University Press, New York, 2010).

[21] D. P. Holmes. Elasticity and Stability of Shape-Shifting Structures. Curr. Opin. Colloid Interface Sci. 40, 118 (2019).